

# Transmission Electron Microscopy Characterization of a Nb Microalloyed Steel for Carburizing at High Temperatures

R.F. de Moraes, A. Reguly, and L.H. de Almeida

(Submitted January 5, 2006)

The carbide particles in AISI 5115 steel modified with added 0.038 wt.% Nb were characterized by means of transmission electron microscopy after simulation of carburizing heat treatments at high temperatures. The advantage of a high-temperature carburizing treatment over the standard 930 °C heat treatment is the significant reduction in the processing time. However, higher carburizing temperature leads to general and abnormal grain growth, which must be avoided by grain-pinning precipitates. The carburizing heat treatment simulations were performed at 950, 1000, and 1050 °C for 1 and 2 h in samples with two prior microstructural conditions: hot rolled and spheroidized. Characterization of the precipitates regarding composition, morphology, size, and distribution was performed using carbon extraction replicas and thin foil specimens. The results confirm the existence of complex Nb carbides. Particle size distribution curves, as log-normal functions, are shown to be extremely important in the interpretation of grain boundary pinning, rather than the mean particle size. The spheroidized samples showed a susceptibility to abnormal grain coarsening.

**Keywords** high-temperature carburizing, niobium precipitates, transmission electron microscopy

## 1. Introduction

The mechanical-metal industry is turning more and more to metallurgical processes for surface hardening of parts and components to obtain the required properties. Together with this demand, questions of automation and efficiency have become of greater importance (Ref 1-3).

Traditionally for components for surface hardening, medium carbon steels with additions of Cr, Ni, and Mo are used, as for example in the AISI steels 4118, 4320, 4620, 5120, and 8620. Temperatures of the conventional processes normally do not surpass 930 °C due mainly to the excessive, prior growth of austenite grains. In some cases, treatments known as “carburizing at high temperature,” at up to 1050 °C, are used for such steels modified with Al, Ti, and/or Nb (Ref 2, 4).

This increase in temperature allows a significant reduction in the process time and therefore is suitable for continuous industrial production lines (Ref 2, 3). Also, at high temperatures, deeper case depths with smoother carbon concentration gradients from the surface to core may be obtained (Ref 3, 5).

Grain boundary pinning during the carburizing process is due to the existence of fine second-phase particles previously precipitated during thermomechanical processing of the steels. The presently accepted viewpoint is that there is an ideal critical size to retard recrystallization and growth of austenite

grains, which contributes to refinement of the final microstructure (Ref 6, 7). This precipitation in austenite can occur at grain boundaries or in the matrix, the latter case being more effective for grain boundary pinning, as precipitation along the grain boundaries could lead to acceleration of the Oswald ripening phenomena.

Nb and Ti are elements that possess a great affinity to C and N. Nb compounds are more soluble than those formed with Ti, they precipitate in the austenite field, and usually result in a fine dispersion of carbonitrides (Ref 8, 9). Solubility of Nb carbide in austenite is mainly a function of temperature. Because Ti nitride is stable at high temperatures, it is also used most effectively to inhibit abnormal grain growth (Ref 10).

The potential for grain growth inhibition is well documented in the literature, and different relationships between the grain diameter and the size and volume fraction of grain pinning precipitates have been proposed (Ref 11-14). The different equations are variations of the classic Zener equation:  $R = 4r/3f$ , where  $R$  is the average grain radius,  $r$  is the average precipitate radius, and  $f$  is the volumetric fraction of the precipitates (Ref 11). From the Zener equation, one can conclude that the smaller the precipitate, the larger its potential to prevent austenite grain growth. In the same way, the smaller the grain size, the larger the volumetric fraction of second-phase precipitates necessary for grain boundary pinning. Some authors consider this relationship to overestimate the extent of grain growth as the values found in practice display a smaller grain size (Ref 12, 13). On the basis of this observation, Cuddy and Raley (Ref 14) showed from the data of other authors a linear relationship between grain size ( $D$ ) and the ratio of the particle diameter ( $d$ ) to the volumetric fraction of the particles ( $f$ ),  $d/f$ .

During cooling or isothermal treatment of steels with grain-controlling carbonitride precipitates, some grains may become unpinned because of growth or dissolution of the precipitates, resulting in abnormal grain growth. The heterogeneity of the

R.F. de Moraes and A. Reguly, Departamento de Engenharia Metalúrgica, Universidade Federal do Rio Grande do Sul, Av. Osvaldo Aranha, 99/610, CEP 90035-190, Porto Alegre, RS, Brazil; and L.H. de Almeida, Programa de Engenharia e Metalúrgica e Materiais, Universidade Federal do Rio de Janeiro, CP 68505, CEP 21945-970, Rio de Janeiro, RJ, Brazil. Contact e-mail: lha@metalmat.ufrj.br.

precipitate distribution can also lead to abnormal grain growth when the ratio of the radius of the particles to the volumetric fraction,  $r/f$ , is locally much smaller than the average value (Ref 15).

In the present work, an evaluation of the microstructural aspects was made through quantification of the sizes of the precipitates of AISI 5115 modified with the addition of Nb, resulting from thermal simulation of carburizing heat treatments at high temperatures (950, 1000, and 1050 °C). This modified steel possesses characteristics that distinguish it from the traditional family of HSLA steels, in that it does not achieve the level of mechanical strength of this class of steel and has the addition of a single precipitation hardening element. However, precipitation did control the grain growth of this steel adequately for carburizing.

To evaluate the size of second-phase precipitates using transmission electron microscopy (TEM) of thin foils, it must be taken into consideration that, when a cut is made during sample preparation, the precipitates on this plane are also severed. In this way, during counting, the diameters of the particle intersections along the cut planes are measured similarly to those in the inner material. It must also be remembered that, for measurement of particle size from extraction replicas, sectioning of particles on a polished surface prepared for film deposition is made in the same way as for thin foil samples. In addition, the distribution of particle sizes will be influenced by the depth of the chemical attack prior to deposition of the extraction film and by the efficiency of the second chemical attack to remove the film. The ideal condition considered in

this calculation would be that all particles that intersect with the polished surface be completely removed from the remaining volume and that they are totally inert to the attack. However, these conditions are very unlikely to occur, and deviation from ideal conditions must be considered. On the other hand, the advantage of using the replication method is that it allows measurement of a large number of samples compared with what would be obtained with observation of a thin foil with the same amount of work. An additional advantage of using replicas for the counting of particle sizes is that it permits analysis of their size distribution. This distribution is spread over a large range of values, and normally the deviation from the standard value is very large, making it impossible to compare samples processed differently. In the present case, the distribution curves for the particle counting by band size displayed a log-normal function (Ref 16). For these reasons, the method has the advantage of comparatively minimizing the errors in measurement, as much from the counting itself as from the inherent nature of the sample preparation process, and allows different microstructural conditions to be compared.

## 2. Materials and Methods

AISI 5115 steel modified with the addition of 0.038 wt.% Nb was in the form of hot-rolled bars, with diameters of 29.50 and 33.34 mm; the chemical composition is shown in Table 1. This material was supplied by Açõs Finos Piratini, Porto Alegre, Brazil.

Groups of these bars in two microstructural conditions, hot

**Table 1 Chemical composition of steel used in this work (wt.%)**

Composition of AISI 5115 standard steel is also shown.

	C	Mn	Si	S <sub>max</sub>	P <sub>max</sub>	Cr	Nb	Ni	Mo	Ti
AISI 5115	0.13-0.18	0.70-0.90	0.15-0.35	0.012-0.035	0.040	0.070-1.05	...	...	...	...
AISI 5115-Nb	0.18	0.95	0.25	0.012	0.008	0.83	0.038	0.14	0.03	0.004

**Table 2 Carburizing simulation heat treatments for both BL and ES microstructural conditions**

Condition	950 °C		1000 °C		1050 °C	
	5 h	6 h	1 h	2 h	1 h	2 h
29.50-BL	Stabilized	Stabilized	Stabilized	<b>Stabilized</b>	Stabilized	<b>Stabilized</b>
29.50-ES	Stabilized	Stabilized	Stabilized	<b>Stabilized</b>	Abnormal growth	<b>Abnormal growth</b>
33.34-BL	Stabilized	Stabilized	Stabilized	Stabilized	Stabilized	Abnormal growth
33.34-ES	Stabilized	Stabilized	Abnormal growth	<b>Abnormal growth</b>	Abnormal growth	Abnormal growth

BL, hot rolled; ES, spheroidized; diameters of bars (mm), 29.50 and 33.34. Abnormal grain growth after heat treatment is indicated as "Abnormal growth," conditions chosen for TEM examination are shown in boldface type.

**Table 3 Distribution characteristics, size, and volumetric fraction of precipitates as well as effect over prior austenite grain caused by the carburizing heat treatment simulations**

Sample	Band size, nm	Average size, nm	Prior austenite grain, ASTM	Volume fraction, %	Distribution of precipitates
BL-29-00	8-89	36	Stabilized	0.70	Homogeneous
ES-29-00	5-100	36	Stabilized	0.73	Homogeneous
BL-29-50	7-156	41	Stabilized	0.71	Homogeneous
ES-29-50	6-135	40	Abnormal growth	0.76	Regions without precipitation
ES-33-00	6-139	22	Abnormal growth	0.72	Regions without precipitation

All samples, according to Table 2, were heat treated for 2 h; "00" indicates 1000 °C, and "50" indicates 1050 °C.

rolled, and spheroidized at 750 °C for 14.8 h, were submitted to heat treatments that simulated thermal cycles in the high-temperature carburizing process at 950, 1000, and 1050 °C, followed by water quenching. Heat treatments were performed at 950 °C for 5 and 6 h and at 1000 and 1050 °C for 1 and 2 h.

The size of the prior austenite grains was examined by light microscopy using polished samples, etched by immersion in an ultrasonic cleaning unit for 15 min, followed by light polishing with 1 μm diamond paste. The etchant solution used contained 100 ml of water, 3 g of picric acid, 10 g of sodium dodecylbenzene, and 5 drops of concentrated hydrochloric acid. Microstructures of the samples after the heat treatment described above were revealed by etching with 3% Nital.

TEM was used to observe the precipitated particles and to evaluate their size, morphology, and distribution. Twenty negatives for each condition (original magnification, 20,000×) were used for particle size measurement. For each condition, ~1000 particles were measured. The TEM samples were taken from the center of the cross section of the bars. Energy-dispersive spectroscopy (EDS) analysis was used for qualitative chemical analysis of the precipitates. Selected-area electron diffraction was also used for identification of precipitates.

The samples were prepared using the method of carbon-film extraction replication. A carbon film was placed on a point of interest of the sample, which had been polished and treated with 5% Nital to expose the particles. To facilitate extraction of the carbon film, cuts in the form of a grid were made, and then the samples were immersed into a solution of 5% Nital. The exposed film was then fixed on a 100 mesh copper grid. Thin foil specimens were also prepared by flat polishing. This is a mechanical polishing step with a diamond lapping film ranging from 6 to 0.5 μm in a low-speed rotary polisher. A disk 3 mm in diameter with an original thickness of 100 μm, previously formed by electro-erosion, was mechanically polished until the region of interest had a thickness <10 μm.

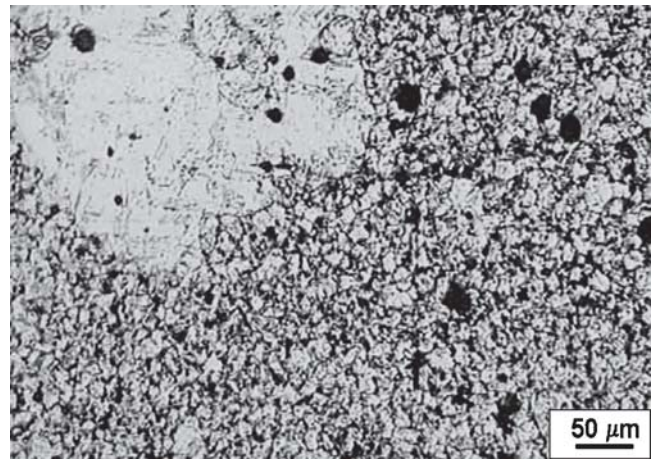
The diameters of the precipitates for each sample, obtained by TEM, were measured individually from the micrograph obtained from different regions using image analysis software. Twenty negative films for each condition (original magnification, 20,000×) were used in these measurements. The volumetric fraction of the precipitates was calculated in the same way using an image analysis program showing the proportion be-

tween the areas of the precipitates and total area of the field analyzed, and also by the classic intercept counting method.

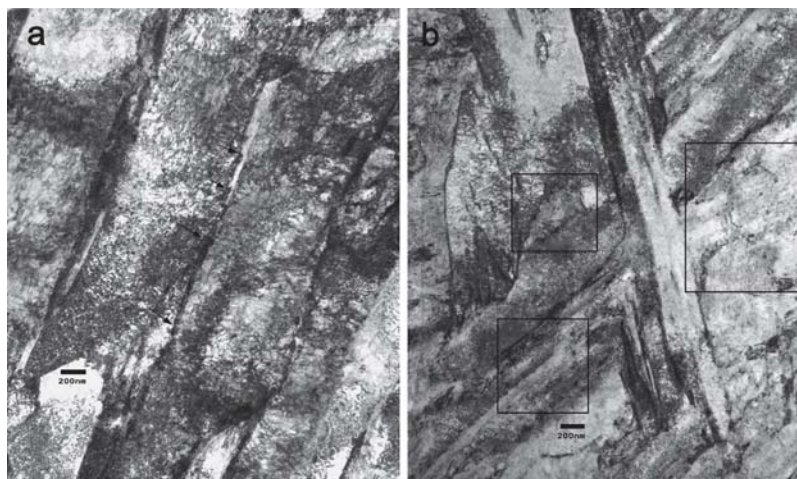
### 3. Results and Discussion

Table 2 shows the heat treatment conditions that simulate the carburizing process for the two different microstructural conditions and indicates which of them showed abnormal grain growth. The cells with gray backgrounds correspond to conditions that were selected for microstructural characterization using TEM.

Measurements of prior austenite grain size of selected samples indicated a uniform size, corresponding to ASTM 12 (Ref 17). After the carburizing simulation heat treatment, abnormal grain growth occurred in some samples, notably at higher temperatures, 1000 and 1050 °C, and in the spheroidized condition as shown in Table 2. The grain size in all samples after simulation, even in the stable regions of those with abnormal grain growth, corresponded to ASTM 10 (Ref 17). Figure 1 illustrates the typical aspect of abnormal grain growth observed in sample BL-33-00.



**Fig. 1** Micrograph showing abnormal grain growth; sample BL-33-00 (light microscope)



**Fig. 2** TEM micrographs obtained using thin foil samples of BL-29-00, bright field: (a) highlighting the aligned precipitates at the martensitic lath interfaces and (b) highlighting the regions with randomly and aligned particle precipitation (bar scales, 200 nm)

The data presented in Table 3, characterizing the particle size and distribution as well as the volume fraction of the particles, were taken from observations of samples prepared by carbon film extraction replication. In this table, conditions where abnormal grain growth can be observed are also indicated. The volumetric fraction measurements show very similar values, for all conditions, of ~0.7%. These values serve only as an indication, not as absolute values, as several errors may be added, such as the choice of particles for counting as well as inherent errors from analysis of the image itself. Another factor is that the analysis was made using a carbon extraction replica, wherein extraction of carbonitride precipitates may not be complete.

Randomly distributed particles can be observed in the matrix using thin foil specimens to the same extent as those distributed at the martensitic lath interfaces. This aligned distribution can also be observed in the matrix and not associated with the martensitic lath interfaces, as highlighted in Fig. 2.

In some of these particles associated with the martensitic lath interfaces, the EDS spectrum obtained showed the presence of Nb. Figure 3 shows the EDS spectrum of Nb carbonitrides obtained using a carbon film extraction replica.

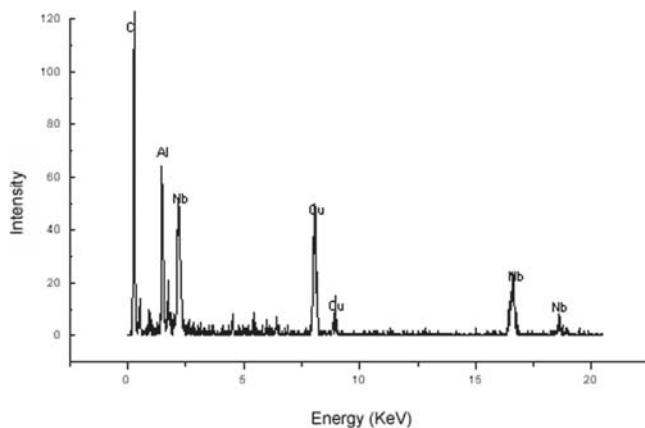


**Fig. 3** EDS spectrum characteristics of precipitated particles containing Nb obtained in carbon replication. The Cu peak comes from the copper grid.

In the analysis using carbon extraction replica specimens, one can observe the presence of large aligned particles (Fig. 4a). The diffraction pattern of the Nb-containing precipitates is also presented showing a lattice parameter  $a_0 = 0.439$  nm. These precipitates appear together with smaller, randomly distributed precipitates (Fig. 4b). This precipitation morphology is very pronounced in the samples where there was no abnormal grain growth.

Analysis using carbon extraction replica specimens showed that, in the conditions without abnormal grain growth, precipitates with characteristics described above were distributed homogeneously over the carbon film while in the conditions with abnormal grain growth there were large regions of the carbon film on which there were no precipitates, as indicated in Table 3.

For size quantification of the precipitates, the particles were classified by band size (results in Fig. 5), which shows the relationship with the thermomechanical history of the samples. Three types of distributions can be identified.

For the two samples with diameters of 29.50 mm with simulation treatments at 1000 °C, BL-29-00 and ES-29-00, the average size of the carbonitrides was similar (Table 3 and Fig. 5).

For the two samples with diameters of 29.50 mm that were heated to 1050 °C, BL-29-50 and ES-29-50, the average size observed in the distribution curves by band size remains similar, between 20 and 30 nm (Table 3). However, a greater number of large-sized particles was observed, which is justified as a tendency for coalescence of the carbonitrides to intensify with an increase in temperature. As a consequence, the average arithmetic size was larger as compared with the other samples with the same diameter, 41 and 40 nm, respectively (Table 3). It is important to emphasize that the sample in the spheroidized condition presented abnormal grain growth while this did not occur with the hot-rolled sample.

From the data available from this work, it is not possible to make any definite conclusion to explain the abnormal grain growth of the spheroidized sample that was treated at 1050 °C for 1 h. It is clear, however, that spheroidization influences the growth and distribution of the precipitate sizes as, even in the sample simulated to 1000 °C, a certain quantity of larger precipitates were noted (Fig. 5). A small percentage of precipitates of size ~100 nm are a consequence of the coarsening of a large

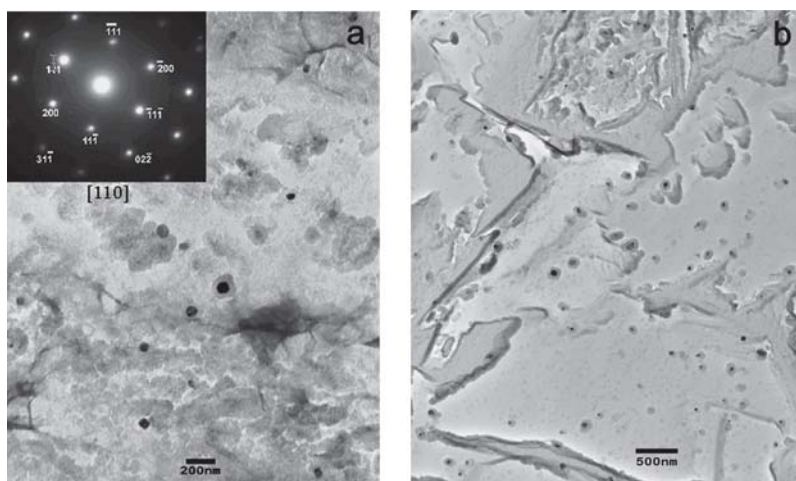


**Fig. 4** Micrographs obtained on carbon extraction replica: (a) larger aligned precipitates (BL-29-00), diffraction pattern of the niobium-containing precipitates according to [011] orientation; (b) randomly distributed precipitates (BL-29-00)

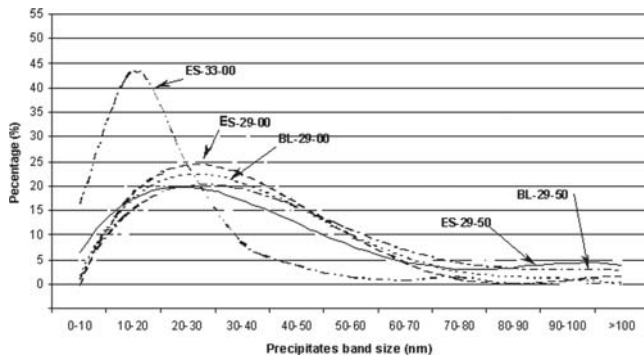


**Fig. 5** Distribution curves by band size of the precipitates found in the analyzed samples

number of finer particles. This growth could produce the regions with a low precipitate density.

The ES-33-00 sample, which had been heat treated to 1000 °C, showed a distribution where the most particles were between 10 and 20 nm, with no coarse particles. The average arithmetic size observed was 22 nm, significantly smaller than the other conditions (Table 3). The history behind the fine distribution in this sample is unknown. However, justification for the abnormal grain growth is related to the small size of the particles, producing a relation,  $4r/3f$ , that is less than that for the other “conditions” and also below the ideal critical size for grain boundary pinning. Note that in the two “conditions” that had abnormal grain growth, the material had gone through the spheroidized thermal treatment before the carburizing heat treatment simulation.

#### 4. Conclusions

- This work shows that AISI 5115 steel, with the addition of 0038 wt.% Nb, may be adequate for high-temperature carburizing as the hot-rolled samples have effective, previous austenite grain boundaries pinned by the niobium carbonitrides.
- Samples that had no abnormal grain growth showed that the average size of the precipitates (20-30 nm), according to the band size distribution curves, was efficient for prior austenite grain boundary pinning. For the spheroidized samples, which did have abnormal grain growth, there are two considerations: presence of a certain quantity of precipitates of size equal to or greater than 90 nm and insufficient number of precipitates of the ideal critical size for pinning.
- TEM characterization and the band size graphs are effi-

cient in themselves for precipitate characterization, showing a relationship between the response of the material to carburizing simulation and grain boundary pinning. The curves show log-normal band size distributions.

#### Acknowledgment

Financial support of CNPq, CAPES, and FAPERGS is gratefully acknowledged. The authors thank Cap. André Pinto from IME for the use the STEM and for helpful discussions.

#### References

1. A.J. Lutz, Carburizing at High Temperatures, *Adv. Mater. Process.*, 1997, **151**(6), p 68AA-68CC
2. “Abnormal Grain Growth of Austenite During Carburizing,” Technical Data Report No. SD8507, Daido Steel, July 1990
3. Heat Treating, *ASM Metals Handbook*, Vol 4, ASM International, 1991, p 348-351
4. T. Kimura and T. Kurebayashi, Niobium in Microalloyed Engineering Steels, Wire Rod and Case Carburized Products, *Proc. Int. Symp. Niobium 2001* (Orlando, FL), Vol 1, p 801-872
5. J.I. Goldstein and A.E. Moren, Diffusion Modeling of the Carburization Process, *Met. Trans. A*, 1978, **9**, p 1515-1525
6. M.G. Akben, I. Weiss, and E.J.J. Jonas, Dynamic Precipitation and Solute Hardening in a V-Microalloyed Steel and 2 Nb Steels Containing High Levels of Mn, *Acta Metall.*, 1981, **29**(1), p 111-121
7. H.-J. Kestenbach and E.V. Morales, Transmission Electron Microscopy of Carbonitride Precipitation in Microalloyed Steels, *Acta Microsc.*, 1998, **7**(1), p 22-33
8. K. Matsukura and K. Sato, Effect of Alloying Elements and Rolling Conditions on the Planar Anisotropy of the R-Value in High Strength Hot-Rolling Steel Sheet for Deep Drawing, *Trans. Iron Steel Inst. Jpn.*, 1981, **21**(11), p 783-792
9. S. Okaguchi, T. Hashimoto, and H. Ohtani, Effect of Nb, V, Ti on Transformation Behavior of HSLA Steel in Accelerated Cooling, *Thermec-88 Physical Metallurgy of Thermomechanical Processing of Steels and Other Metals Conf.*, Vol 1 (Tokyo, Japan), The Iron and Steel Institute of Japan, June 1988, p 330-336
10. J. Zrník, T. Kvackj, D. Sripinproach, and P. Sricharoenchai, Influence of Deformation Conditions on Structure Evolution in Nb-Ti Microalloyed Steel, *J. Mater. Process. Technol.*, 2003, **133**(1-2), p 236-242
11. C. Zener, Theory of Growth of Spherical Precipitates from Solid Solution, *J. Appl. Phys.*, 1949, **20**(10), p 950-953
12. T. Gladman, *Fundamentals and Applications of Microalloying Forging Steels*, 1st ed., C.J. Van Tyne, G. Krauss, and D.K. Matlock, Ed., TMS, 1996, p 3-16
13. T. Gladman and F.B. Pickerin, Grain-Coarsening of Austenite, *J. Iron Steel Inst.*, 1967, **205**(6), p 653-664
14. L.J. Cuddy and J.C. Raley, Austenite Grain Coarsening in Microalloyed Steels, *Metall. Trans. A*, 1983, **14**(10), p 1989-1995
15. J.C. Bruno and P.R. Rios, The Grain Size Distribution and the Abnormal Grain Growth of Austenite in an Eutectoid Steel Containing Niobium, *Scr. Metall. Mater.*, 1995, **32**(4), p 601-606
16. M.F. Ashby and R. Eberly, On the Determination of the Number, Size, Spacing and Volume Fraction of Spherical Second-Phase Particles from Extraction Replicas, *Trans. AIME*, 1966, **236**(10), p 1396-1404
17. “Determining the Standard Grain Size,” E112, *Annual Book of ASTM Standards*, ASTM, 1985